

Influence of Chitosan Nanoparticles as the Absorption Enhancers on Salvianolic acid B *In vitro* and *In vivo* Evaluation

Xin Jin, Shi-bing Zhang, Shi-meng Li, Ke Liang¹, Zeng-yong Jia

Department of Pharmacy, The Suqian First Hospital, Suqian, Jiangsu 223800, ¹Depratment of Pharmacy, The First Affiliated Hospital of Soochow University, Suzhou, Jiangsu 215006, China

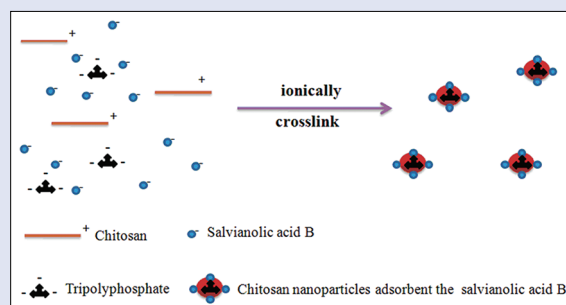
ABSTRACT

Background: Salvianolic acid B (SalB) represents the most abundant and bio-active phenolic constituent among the water-soluble compounds of *Salvia miltiorrhiza*. But the therapeutic potential of SalB has been significantly restricted by its poor absorption. **Methods:** In this study, chitosans (CS) and CS nanoparticles (NPs) with different molecular weights (MWs), which have influence on the absorption of SalB, was also investigated. **Results:** As a preliminary study, water-soluble CS with various MWs (3, 30, 50, and 100 kDa) was chosen. We investigated the MW-dependent Caco-2 cell layer transport phenomena *in vitro* of CS and NPs at concentrations (4 µg/ml, w/v). SalB, in presence CS or NPs has no significant toxic effect on Caco-2 cell. As the MW increases, the absorption enhancing effect of CS increases. However, as the MW decreases, the absorption enhancing effect of NPs increases. The AUC_{0-12h} of the SalB-100 kDa CS was 4.25 times greater than that of free SalB. And the AUC_{0-12h} of the SalB-3 kDa NPs was 16.03 times greater than that of free SalB. **Conclusion:** CS and NPs with different MWs as the absorption enhancers can promote the absorption of SalB. And the effect on NPs is better than CS.

Key words: Absorption enhancer, bioavailability, Caco-2 cell model, chitosan, chitosan nanoparticles, molecular weight, salvianolic acid B

SUMMARY

- Formation mechanism for NPs



Correspondence:

Dr. Ke Liang, The First Affiliated Hospital of Soochow University, 188 Shizi Road, Suzhou, Jiangsu, 215006, China.

E-mail: keliang_sz@163.com

Dr. Zeng-yong Jia, The Suqian First Hospital, 120 Suzhi Road, Suqian, Jiangsu, 223800, China.

E-mail: zengyongjia_sq@163.com

DOI : 10.4103/0973-1296.176047

Access this article online

Website: www.phcog.com

Quick Response Code:



INTRODUCTION

Danshen, the dried root of *Salvia miltiorrhiza*, is a widely used traditional herb in China to improve body functions. Salvianolic acid B [SalB, structure shown in Figure 1a] represents the most abundant and bioactive phenolic constituent among the water-soluble compounds of Danshen.^[1] Studies have shown that SalB can elicit endothelium-dependent vasodilation,^[2] lower blood pressure in hypertension,^[3] and improve regional cerebral blood flow and prohibit platelet aggregation.^[4]

SalB has attractive pharmacological activities; however, the treatment of SalB has been significantly restricted by its poor bioavailability. Generally, hydrophilic compounds transport across the intestinal barrier via paracellular pathway.^[5] The presence of tight junctions between the epithelial cells will limit absorption of SalB when the paracellular pathway occupies less than 0.1% of the total surface area of the intestine epithelium.^[6] It is difficult to find the suitable delivery to increase SalB absorption due to its hydrophilic.

Due to the special features of adhering to the mucosal surface and transiently opening the tight junctions between epithelial cells, Chitosan [CS, Figure 1b] have been used as an absorption assistance of hydrophilic molecules.^[7,8] Meanwhile CS can be ionically cross linked with multivalent anions such as tripolyphosphate [TPP, Figure 1c] to form CS nanoparticles (NPs). This process, known as ionic gelation, has some advantages since it is a mild process resulting in NPs with low sizes and has been proven to encapsulate different lipophilic, biological, and active compounds.^[9,10]

Although numerous literatures are available on CS and NPs, the absorption relationships between NPs with different molecular weights (MWs) have not been reported.^[11,12] Meanwhile, to the best of our knowledge, NPs was first chosen as the absorption enhancer to absorb the hydrophilic SalB, which is charged negatively. Caco-2 cell culture model is used to investigate drug absorption and is recognized by Food and Drug Administration (FDA) as viable models of human intestinal absorption.^[13] The tight-junctions of Caco-2 monolayer formed at the apical side of the monolayer can discriminate the transcellular and paracellular transport of drugs across the epithelial layer.^[14] The drug permeability to Caco-2 monolayer is expected to correlate well with that of the intestinal membrane *in vivo*. Some reports have shown the possibility that the oral absorption of drugs in human body can from their permeability to Caco-2 monolayer.^[15,16] Hence, Caco-2 cell model, which measures the permeability, is used to indicate the absorption in

This is an open access article distributed under the terms of the Creative Commons Attribution-NonCommercial-ShareAlike 3.0 License, which allows others to remix, tweak, and build upon the work non-commercially, as long as the author is credited and the new creations are licensed under the identical terms.

For reprints contact: reprints@medknow.com

Cite this article as: Jin X, Zhang Sb, Li Sm, Liang K, Jia Zy. Influence of chitosan nanoparticles as the absorption enhancers on salvianolic acid B *In vitro* and *In vivo* evaluation. Phcog Mag 2016;12:57-63.

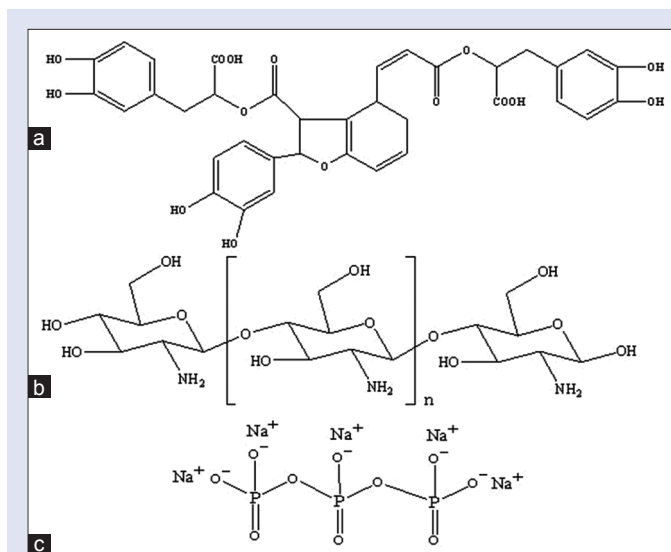


Figure 1: (a) Salvianolic acid B (b) chitosan and (c) sodium tripolyphosphate

this article. Furthermore, *in vivo* pharmacokinetic profiles after oral administration were evaluated to determine the effect of the CS and NPs on absorption of SalB.

MATERIALS AND METHODS

Instruments and materials

Rosmarinic acid (99.8%) and SalB (99.5%) were purchased from the National Institute for the Control of Pharmaceutical and Biological Products (NICBP, Beijing, China). Water-soluble CS with various MWs (3, 30, 50, and 100 kDa) were supplied by KITTOLIFE (Seoul, Korea). Cloned Caco-2 TC7 cells were a generous gift from Dr. Ming Hu of INSERM U178 (Houston, TX). Sodium TPP was purchased from Merck (Darmstadt, Germany). 3-[4,5-dimethylthiazol-2-yl]-2,5-diphenyl tetrazolium bromide (MTT) and Hank's balanced salt solution (HBSS; powder form) were purchased from Sigma-Aldrich (St. Louis, MO). Milli-Q water (Millipore, Bedford, MA) was used throughout the study. All the reagents were of analytical grade, except acetonitrile and methanol, which were chromatographic grade (Merck Company Inc., UN).

Animal experiments

Male Sprague-Dawley rats weighing 200–250 g were obtained from the SLAC Laboratory Animal Center of Shanghai (Shanghai, China). The animals were housed under standard conditions of temperature, humidity, and light. Food and water were provided *ad libitum*. The rats were fasted overnight before the day of the experiment. All animal experiments procedures were conducted according to the Guiding Principles in the Use of Animals in Toxicology.

Preparation and characterization

NPs were formed as complex electrostatic interactions between the positively charged copolymers and the negatively charged TPP under mild conditions.^[17] Therefore, CS was dissolved in acetic acid solution (1.0% volume/volume). The concentration of acetic acid in aqueous solution was 1.5 times greater than of CS. Then, 20 ml sodium TPP solution (1.0 mg/mL) was added to CS solution. A nano suspension was obtained upon the addition of the sodium TPP aqueous basic solution to the CS aqueous solution via mechanical stirring of 1000 rpm at room temperature. And homogenized by passing three cycles through a high-pressure homogenizer (Avestin Em-C3, Ottawa, Canada) at 200 bar and 25°C to obtain an opalescent

dispersion of the NPs. Particle size distribution (Z-average), polydispersity index (PDI), and zeta potential of the dispersions were determined by photon correlation spectroscopy (Zetasizer Nano-ZS Malvern Instruments, Worcestershire, UK). Measurements were performed at 25°C, and the results were showed as the mean of three successive measurements of at least three independent samples. Each sample was diluted with distilled water to adjust the signal level. Measurements were carried out in dilute 1% acetic acid medium, and each sample was measured in triplicate. Then the morphological evaluation was performed using transmission electron microscopy (TEM; JEM-1200EX, Japan).^[18,19]

MTT assay

The cytotoxic effects on Caco-2 cells were determined with MTT assay.^[20] Caco-2 cells used for MTT assay were plated in 96 well cell culture plates at a density 2×10^4 cells/well and preincubated for 24 h before treatment. Then the cells were treated with samples (10 μ mol SalB, in the presence CS or NPs with different MW) in serum-free medium (pH 5.5) for 24 h. The solutions were removed and fresh cell culture medium was added after treatment. Then the cells were incubated for 4 h to stabilize them. After stabilization, the cells were incubated with MTT (0.1 mg/ml MTT in serum-free medium) for 4 h. Finally, the medium was removed, and the resulting formazan crystal was dissolved with 100 μ l DMSO per well. The cell relative viability (%) was calculated by using a microplate reader (Universal Microplate Analyzer, Model AOPUS01 and AI53601, Packard BioScience, CT, USA). Viability of nontreated control cells was arbitrarily defined as 100%.^[21]

$$\text{Relative cell viability} = \frac{(\text{OD}_{550, \text{sample}} - \text{OD}_{550, \text{blank}}) \times 100}{(\text{OD}_{550, \text{control}} - \text{OD}_{550, \text{blank}})} \quad \text{Equation (1)}$$

Where $\text{OD}_{550, \text{blank}}$ the absorption values of culture plates without cells at 550 nm, $\text{OD}_{550, \text{control}}$ the absorption values of samples that were treated blank HBSS at 550 nm, $\text{OD}_{550, \text{sample}}$ the absorption values of samples that were treated experimental samples at 550 nm.

Permeability studies in the Caco-2 cell culture model

For the transport assay, Caco-2 cell (passage 38) were seeded on Transwell® (Biotechnology Co., Ltd. Shanghai Brilliance Cup) inserts in six well Transwell plates, which have a surface area of 4.2 cm², at a density of 100,000 cells/cm² in growth medium (Dulbecco's modified Eagle's medium supplemented with 10% fetal bovine serum). The quality control criteria were based on previously published reports.^[22] The culture medium was changed every 24 h. Cells were cultured for at least 21 days at 37°C, 90% humidity, and 5% CO₂ before they were used for the transport studies between days 21 and 23.^[23]

The transport of samples across the Caco-2 cell monolayer at pH 5.5 was studied. Caco-2 monolayers grown in Transwell® (6-well) plates were used for transport researches when they had differentiated and the monolayer was intact, as checked by measuring transepithelial electrical resistance (TEER).^[24] The cell monolayer was washed thrice with blank HBSS (at pH 5.5 and 37°C) before the experiment. The TEER values of the cell monolayer measured were more than 350 $\Omega \cdot \text{cm}^2$. The monolayer was incubated using blank HBSS (pH 5.5) for 1 h, then aspirated incubation medium. A solution containing 10 μ mol SalB (in the presence CS or NPs with different MW) was then fitted on the apical of the monolayer. By using Ultra performance liquid chromatography (UPLC), the amounts of transported compound were measured as a function of time. Receiver samples (400 μ l) and donor samples (400 μ l) were taken in triplicate at different times, then 400- μ l drug donor solution were added to the donor side or 400 μ l of blank buffer were added to the receiver side. Each was given at the same concentration (10 μ M) to compare the permeability of

SalB, and the samples were collected at 0, 1, 2, 3, and 4 h after incubation. To each transport sample (400 µl), the addition of rosmarinic acid (20 µM) was as a preservative and internal standard. The resulting mixtures were swirled for 30 s and centrifuged at 15,000 rpm for 15 min. The supernatant was analyzed by UPLC within 24 h. The permeability of SalB was calculated using the following equation:

$$P_{app} = \frac{V}{S \times C} \times \frac{dc}{dt} \times \frac{1}{S \times C} \times \frac{dm}{dt} \quad \text{Equation (2)}$$

Where V is the volume of the receiver (typical volume 2.5 mL), S is the surface area of the cell monolayer (typical surface area 4.2 cm²), C is the initial concentration, $\frac{dC}{dt}$ is the rate of concentration change on the receiver side, and $\frac{dM}{dt}$ is the rate of drug transport. The rate of drug transport was obtained by linear regression analysis.

TEER experiments

Caco-2 cell layers revealing TEER $\geq 350 \Omega \cdot \text{cm}^2$ were used in these experiments. Cell medium was removed and replaced with HBSS (buffered at pH 5.5 with HEPES on the apical and basolateral sides of the cell layers) before sample application. Cells were equilibrated in HBSS (incubated at 37°C, 5% CO₂) for 1 h, then TEER was measured, which was treated as the baseline TEER. NPs and CS (visually transparent in HBSS at pH 5.5) were then applied to the apical side of the cell layers, following which cells were incubated with the samples for 4 h. TEER was measured at times 0, 1, 2, 3, and 4 h (in the presence of the tested samples, in HBSS) following the sample application. Background TEER of the filter (100–110 $\Omega \cdot \text{cm}^2$) was subtracted from the measurements under all conditions. All samples were measured in triplicate.

The change on TEER meaning of the cell monolayer was measured with a Millicell®-Electrical Resistance System (Millipore Corp., Bedford, MA).

Pharmacokinetic studies

Male rats were divided randomly into nine groups for administration of a single dose of SalB or SalB CS of different MW or SalB NPs of different MW. The nine groups of rats were administered oral doses equivalent to 500 mg/kg of SalB. To determine the serum drug concentrations and calculate the pharmacokinetic parameters, blood samples were collected at 0, 10, 15, 20, 30, 45, 60, 90, 120, and 240 min after dosing. The blood samples were centrifuged at 3000 rpm for 10 min, and then the supernatants were collected into tightly sealed plastic tubes (containing a heparin sodium anticoagulation solution). We added 200 µL of an internal standard working solution (5 µg/mL rosmarinic acid in acetonitrile) to 200 µL of the plasma sample, and 800 µL of acetonitrile was then added to the mixture and vortexed for 30 s to precipitate the protein. The resulting mixture was centrifuged at 13,000 rpm for 15 min at 4°C. One milliliter of the upper organic phase was transferred to another tube and evaporated to dryness at 25°C using a Thermo Savant SPD 2010 Speed Vac System (Thermo Electron Corporation, Waltham, MA). The residue was dissolved in 100 µL of methanol and vortex-mixed for 1 min. After centrifugation at 15,000 rpm for 15 min, 20 µL of the supernatant was injected into UPLC system for analysis.

Analytical methods

UPLC was used to detect SalB in the transport samples obtained in the Caco-2 model. The conditions for UPLC analysis of SalB in the transport samples were as follows: System, Waters Acquity UPLC with a photodiode array detector and Empower software (Waters, Milford, MA); column, Acquity UPLC BEH C18, 1.7 µm, 2.1 × 50 mm (Waters). The UPLC elution condition was optimized as follows: 0–4 min (acetonitrile: Water containing 0.1% AcH = 40:60); flow rate 0.4 mL/min; column temperature 35°C; wavelength 286 nm; and injection volume 8 µL. The

retention time for SalB was 1.69 min. The retention time for rosmarinic acid (the internal standard) was 2.61 min.

Statistical analysis

All experiments were performed at least in triplicate. Data were presented as the mean ± standard deviation. Student's *t*-test was used to analyze the data. A two-tailed *t*-test (Microsoft Excel®) was used to identify significant differences (*P* < 0.05) compared with the controls.

RESULT AND DISCUSSION

Characterization of the NPs

The surface morphology and shape of the NPs were observed by scanning electron microscopy. The NPs were almost spherical, with a regular shape [Figure 2]. The particle size, size distribution, and zeta potentials of the NPs were also detected, as shown in Table 1. The NPs ranged from 100 to 300 nm in size with different MWs, and the PDI was less than 0.2. The particles had a relatively narrow size distribution and all of them had strong positive charge. The size measured in hydrated state is proposed to be a little higher than the size measured by TEM method.^[25] In this study, the results were based on the depiction of the size of dried state (actual diameter) by TEM versus hydrated state (hydrodynamic diameter) measured by light scattering.

Cytotoxicity test

The cytotoxicity of SalB, in the presence CS or NPs was assessed by MTT assay on the Caco-2 cell line. SalB, in the presence CS or NPs have no toxic effect on applied cells, and the effect was observed, as in Figure 3.

The effect on *in vitro* absorption

The *in vitro* stability of NPs at different environments of the gastrointestinal tract was different. According to reference,^[26] the morphology of the NPs at pH range of 2.5–6.6 was spherical in shape with a smooth surface; otherwise they became unstable and subsequently broken apart. Therefore pH 5.5 was used *in vitro* absorption, which was available in the intestinal environment. The effect of CS MW on the permeability of SalB through the differentiated Caco-2 cell layer grown on a permeable filter support was examined. The apical to basolateral transepithelial passage of SalB is presented in Table 2, from which we can see that the permeation of SalB through the

Table 1: Physico-chemical properties of NPs (n=3)

Samples	Average size (nm)	Zeta potential (mV)	PDI
3 kDa NPs	103.4±9.2	+44.5±3.2	0.132±0.012
30 kDa NPs	156.7±11.3	+41.4±2.6	0.147±0.012
50 kDa NPs	203.1±13.7	+43.7±4.1	0.165±0.016
100 kDa NPs	294.5±23.4	+40.6±3.8	0.174±0.017

PDI: Polydispersity index; NPs: Nanoparticles

Table 2: Permeability of SalB combine with different molecular weight of CS or NPs

Samples	Papp (10 ⁻⁶ cm/s)
SalB	0.54±0.07
3 kDa CS	1.26±0.11
30 kDa CS	1.45±0.09
50 kDa CS	1.92±0.13
100 kDa CS	2.39±0.15
3 kDa NPs	10.1±0.78
30 kDa NPs	8.35±0.55
50 kDa NPs	7.73±0.62
100 kDa NPs	6.92±0.43

SalB: Salvianolic acid B; NPs: Nanoparticles; CS: Chitosans; Papp: Apparent permeability coefficient

Caco-2 cell layer was changed and depends on the CS MW at 4 $\mu\text{g/ml}$, w/v concentrations. CS achieved good penetration on the Caco-2 cell layer in a MW-dependent manner. The different transport phenomena caused the different values of apparent permeability coefficient (Papp). The relatively high Papp value of 2.39×10^{-6} cm/s was calculated from the CS 100 kDa penetration data. By decreasing CS MW, decreased Papp values of 1.92×10^{-6} cm/s, 1.45×10^{-6} cm/s, and 1.26×10^{-6} cm/s were obtained by CS 50 kDa,

CS 30 kDa, and CS 3 kDa treatment, respectively. The fastest transport was inspected with CS 100 kDa. The penetration rates enhanced as the MW increased. There was more than 4.43-times enhanced transport observed with CS 100 kDa by 4 h treatment when compared with free SalB transport. Meanwhile the different transport phenomena of NPs may result from different mechanisms. As the MW increased at concentrations (4 $\mu\text{g/ml}$, w/v), average size of NPs was increased may conduct the decreasing penetration rates. The relatively high Papp value of 10.1×10^{-6} cm/s was calculated from the NPs 3 kDa permeability data. By increasing CS MW, decreased Papp values of 8.35×10^{-6} cm/s, 7.73×10^{-6} cm/s, and 6.92×10^{-6} cm/s were obtained by NPs 30 kDa, NPs 50 kDa, and NPs 100 kDa treatment, respectively. The permeability of NPs 3 kDa was 18.70 and 4.23 times enhanced, while that of free SalB and CS 100 kDa.

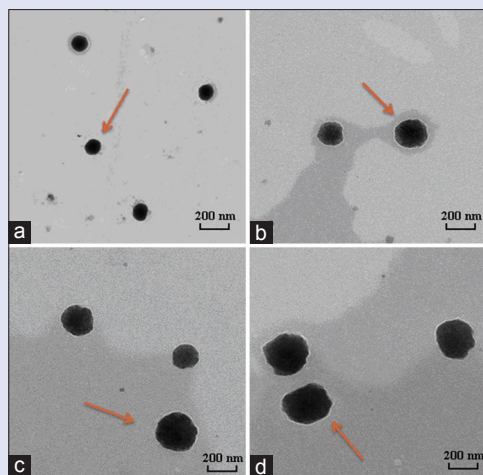


Figure 2: Electron micrographs of NPs adsorbent the SalB. And the NPs were consisted of different molecular weight (MW) of chitosan. MW was 3 kDa (a), 30 kDa (b), 50 kDa (c), and 100 kDa (d), respectively

TEER experiments

Evaluation of the CS and NPs in opening tight junctions was conducted *in vitro* in Caco-2 cell monolayer. Transport experiments were performed using the HBSS (at pH 5.5) medium. And the penetration of compact junction in the Caco-2 cell monolayer was monitored by TEER measurements. The records of TEER were calculated as a percentage relative to baseline TEER (measured just prior to experiment initiation) and plotted versus exposure time.

The effect of CS or NPs at concentrations (4 $\mu\text{g/ml}$, w/v) on the TEER of the Caco-2 layers are presented in Figure 4 (Figure 4a and b for CS and NPs, respectively). Both profiles exhibited a typical pattern of a steep decrease in TEER for all the samples applied. It might be that the CS and NPs with a positive surface charge could reduce the TEER of Caco-2 cell monolayer effectively. After removal of the CS or NPs, which was incubated, a slow increase in TEER was observed. This observation was

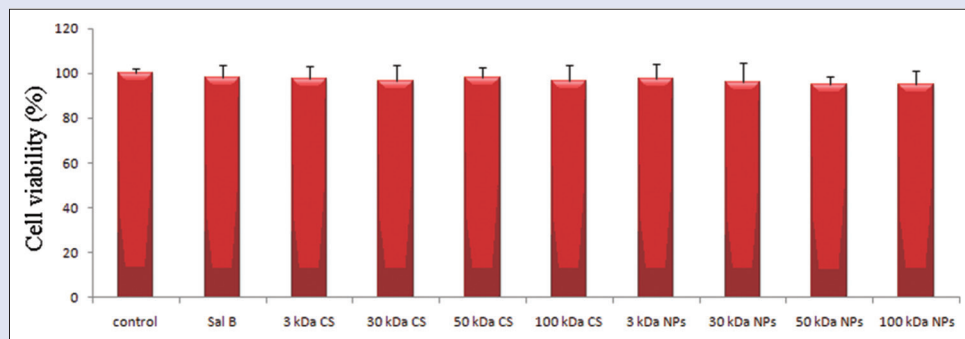


Figure 3: The effect of salvianolic acid B in the presence chitosans or nanoparticles on the viability of Caco-2 cell ($n = 6$)

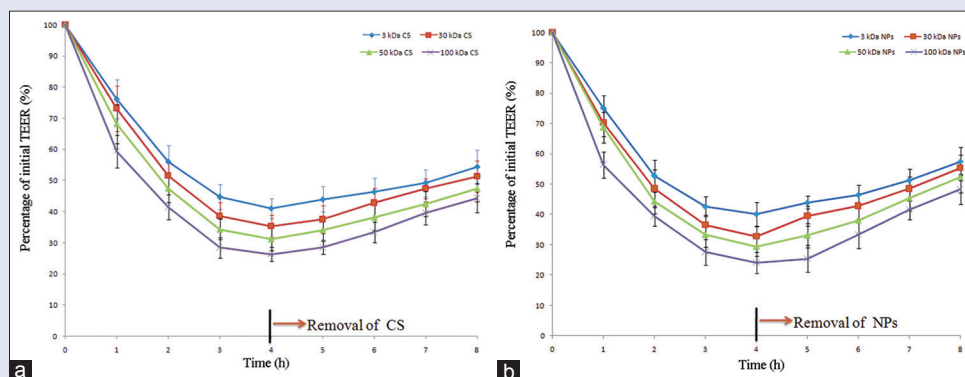


Figure 4: Effects of the chitosans and nanoparticles on the transepithelial electrical resistance values of Caco-2 cell monolayer at pH 5.5. ($n = 3$ for each studied group, a CS b NPs)

obviously more remarkable. In contrast, such results were not observed for the control group without incubation with CS or NPs.

On one hand, the CS samples led to MW-dependent decreases in TEER with 1 h of exposure, with TEER falling to 76.11%, 73.12%, 68.23%, and 59.35% at exposure CS MW of 3 kDa, 30 kDa, 50 kDa, and 100 kDa, respectively [Figure 4a]. The effect stabilized after 4 h with the TEER values recorded at 44.69%, 38.64%, 34.34%, and 28.46%, for the respective MW at 4 h. And the effect of NPs was the same as CS.

On the other hand, the continuous decrease in the TEER values reached around 30% of initial values at 4 h after treatment. And the same phenomenon was observed on the NPs. After the removal of CS or NPs and supply of fresh culture medium, the TEER values started to increase. At 4 h after treatment of fresh culture medium, the TEER values were completely recovered to around 50% of initial levels. Therefore, both CS and NPs had reversibility of opening tight junctions.

Pharmacokinetic studies

We assessed the oral bioavailability of the SalB in rats and compared it with the SalB-CS and SalB-NPs. The mean SalB plasma concentration versus time plots for nine samples equivalent to 500 mg/kg doses of SalB orally administered to rats ($n = 6$) are shown in Figure 5. A summary of the statistical analysis is shown in Table 3. The average values for maximum concentration and time to maximum concentration after oral administration of SalB were 2.73 $\mu\text{g/mL}$ and 28.14 min, respectively, while those after oral administration of the SalB-3 kDa NP were 49.78 $\mu\text{g/mL}$ and 59.14 min, respectively. The average $\text{AUC}_{0-\infty}$ of the SalB-3 kDa NP in rats was 184.51 $\mu\text{g}\cdot\text{min/L}$, which was significantly higher than that of the free SalB. The $\text{AUC}_{0-\infty}$ of the SalB-3 kDa NP was 16.03 times greater than that of free SalB. The size of SalB-NP decreased as the MW of CS. And the relative bioavailability of SalB increased with a decrease in the size of the SalB-NP. Meanwhile, the time to maximum concentration values of SalB significantly decreased as forming the SalB-NPs. But there is no significant difference between SalB-NP.

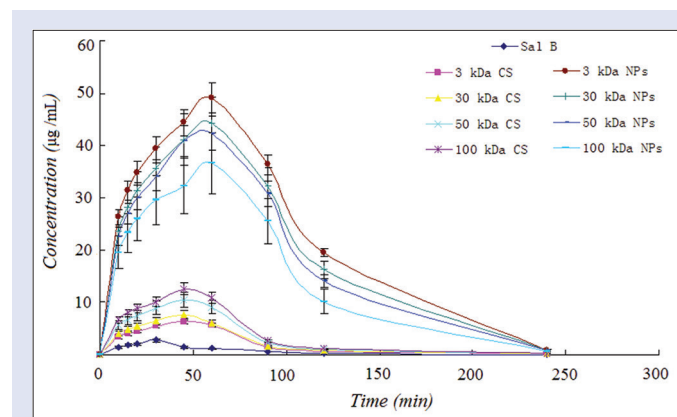


Figure 5: Effects of the chitosans and nanoparticles on the transepithelial electrical resistance values of Caco-2 cell monolayer at pH 5.5. ($n = 3$ for each studied group)

Moreover, the average $\text{AUC}_{0-\infty}$ of the SalB-100 kDa CS in rats was 48.86 $\mu\text{g}\cdot\text{min/L}$, which was significantly higher than that of the free SalB. The $\text{AUC}_{0-\infty}$ of the SalB-100 kDa CS was 4.25 times greater than that of free SalB. The relative bioavailability of SalB increased with an increase in the MW of CS. Interestingly, the time to maximum concentration values of SalB-CS were also decreased. And there is also no significant difference between SalB-CS.

The tight gastrointestinal epithelium represents major barriers to drug delivery. Therefore, various oral delivery strategies have been examined to overcome these difficulties. This study described the existence of a range of CS-based delivery systems with considerable potential for oral application.

Several proprietary properties such as biocompatibility, biodegradability, and nontoxicity offer CS boundless potentials for pharmaceutical applications.^[27] In the biopharmaceutical opinion, CS has an enhancement of paracellular drug transport via transient opening of compact junction between epithelial cells.

In the present study, it was proposed that the mechanism of absorption enhancing effect of CS was an effect on tight junctions across ionic interactions with negatively charged groups of glyocalix and no apparent toxicity during long-term therapy.^[28] Furthermore, the reference reported that the absorption enhancing effect of CS on the improvement of the intestinal absorption was affected by their concentrations, which was observed at relatively higher concentration.^[29] However, in this article, the low concentration of CS (4 $\mu\text{g/mL}$, w/v) was found to have a great absorption enhancing effect on SalB. The reasons that the absorption enhancing effects of CS might be because of interactions with negatively charged groups of glyocalix and the low viscosity of CS at 4 $\mu\text{g/mL}$.^[30]

Meanwhile, CS-NPs have been developed by the ionotropic gelation method using TPP anions.^[31] The purpose of CS-NPs was to provide a nanoscale system adsorbent SalB (negatively charged substrates), for its application. However, the trends in TEER and PapP values develop are not in parallel between CS and NPs as they reflected the different functional properties. NPs have the same effect as CS on opening the tight junctions. But the absorption enhancing effect by NPs was significantly larger than CS. In addition, it was proposed that aside the mechanisms possesses by CS, there was another possible and crucial mechanism responsible for NPs improving drug absorption is endocytosis.^[32] NPs showed different mechanisms of distribution and cellular uptake when compared with CS. The strong positive charge of NPs makes it possible to bind negatively charged substrates, such as lipids, in intestinal epithelial cells. It was reported that adhesion of NPs to the cell surface is a prerequisite to generate the interaction of cells with NPs. After adhesion, the internalization of NPs in cells may occur by fluid phase endocytosis or phagocytosis. Cellular uptake of NPs is a significant concern in absorption enhancement.

NPs can promote the drug delivery across cell surface barriers and result in opening of the tight junctions between epithelial cells transiently. Then, CS just has the function of opening of tight junction. Based on the above results, we drew the schematic diagram of intestinal SalB transport in presence of CS or NPs [Figure 6].

Table 3: Pharmacokinetic parameters of SalB, SalB-CS, and SalB-NPs orally in rats ($n=6$)

Parameters	SalB	3 kDa CS	30 kDa CS	50 kDa CS	100 kDa CS	3 kDa NPs	30 kDa NPs	50 kDa NPs	100 kDa NPs
AUC_{0-t} ($\mu\text{g}\cdot\text{min/L}$)	10.23 \pm 1.01	22.57 \pm 2.14	28.61 \pm 2.41	37.57 \pm 3.71	45.38 \pm 3.97	180.23 \pm 20.01	167.23 \pm 18.56	145.73 \pm 15.46	130.43 \pm 13.01
$\text{AUC}_{0-\infty}$ ($\mu\text{g}\cdot\text{min/L}$)	11.51 \pm 1.49	23.47 \pm 2.49	29.07 \pm 2.82	39.22 \pm 3.47	48.86 \pm 4.16	184.51 \pm 24.45	172.33 \pm 19.26	150.51 \pm 20.11	135.81 \pm 16.58
T_{\max} (min)	28.14 \pm 4.13	43.14 \pm 5.01	44.26 \pm 4.33	46.32 \pm 2.98	44.78 \pm 4.36	59.14 \pm 5.71	58.29 \pm 4.56	60.45 \pm 5.51	61.96 \pm 4.99
C_{\max} ($\mu\text{g/mL}$)	2.73 \pm 0.22	6.27 \pm 0.79	7.644 \pm 0.93	10.42 \pm 1.41	12.56 \pm 2.05	49.78 \pm 6.77	44.23 \pm 5.29	42.31 \pm 5.21	36.58 \pm 4.27

The data are presented as the mean \pm SD. AUC: Area under concentration-time curve; T_{\max} : Time to maximum plasma concentration; C_{\max} : Maximum plasma concentration; SalB: Salvianolic acid B; CS: Chitosans; NPs: Nanoparticles; SD: Standard deviation

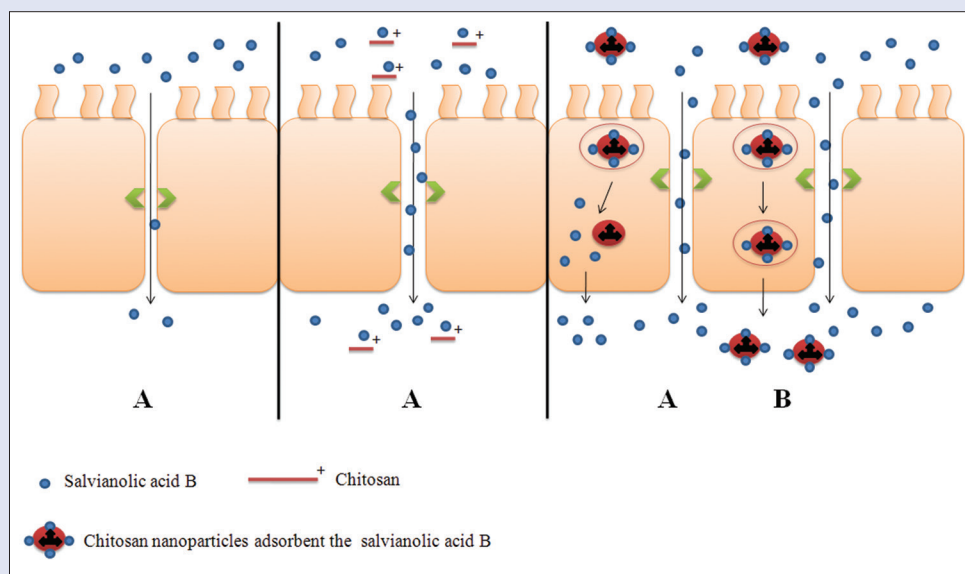


Figure 6: Schematic diagram of SalB for intestinal transportation. The proposed mechanisms include: Paracellular transport (A) and fluid phase endocytosis (B) are ready for salvianolic acid B absorption

CONCLUSION

It was concerned that CS NPs had a more positive effect of absorption enhancement on Caco-2 cell model when compared with CS. And the penetration rates on the Caco-2 cell layer enhanced as the CS's MW increased. In addition, our results indicate that NPs of a smaller size improve the oral absorption of salB. However, the mechanism that CS NPs had an absorption enhancement needs to be further investigated.

Acknowledgments

This study was financially supported by the National Natural Science Foundation of China (No 81403119).

Financial support and sponsorship

Nil.

Conflicts of interest

There are no conflicts of interest.

REFERENCES

- Zhou L, Zuo Z, Chow MS. Danshen: An overview of its chemistry, pharmacology, pharmacokinetics, and clinical use. *J Clin Pharmacol* 2005;45:1345-59.
- Kamata K, Iizuka T, Nagai M, Kasuya Y. Endothelium-dependent vasodilator effects of the extract from *Salviae miltiorrhizae* radix. A study on the identification of lithospermic acid B in the extracts. *Gen Pharmacol* 1993;24:977-81.
- Kamata K, Noguchi M, Nagai M. Hypotensive effects of lithospermic acid B isolated from the extract of *Salviae miltiorrhizae* radix in the rat. *Gen Pharmacol* 1994;25:69-73.
- Tang MK, Ren DC, Zhang JT, Du GH. Effect of salvianolic acids from Radix *Salviae miltiorrhizae* on regional cerebral blood flow and platelet aggregation in rats. *Phytomedicine* 2002;9:405-9.
- Schipper NG, Vårum KM, Stenberg P, Ocklind G, Lennernäs H, Artursson P. Chitosans as absorption enhancers of poorly absorbable drugs 3: Influence of mucus on absorption enhancement. *Eur J Pharm Sci* 1999;8:335-43.
- Zhou L, Chow MS, Zuo Z. Effect of sodium caprate on the oral absorptions of danshensu and salvianolic acid B. *Int J Pharm* 2009;379:109-18.
- Zhou W, Zhu XX, Yin AL, Cai BC, Wang HD, Di L, *et al.* Effect of various absorption enhancers based on tight junctions on the intestinal absorption of forsythoside A in Shuang-Huang-Lian, application to its antiviral activity. *Pharmacogn Mag* 2014;10:9-17.
- Barakat NS, Almurshedi AS. Design and development of gliclazide-loaded chitosan microparticles for oral sustained drug delivery: *In-vitro/in-vivo* evaluation. *J Pharm Pharmacol* 2011;63:169-78.
- Prego C, Fabre M, Torres D, Alonso MJ. Efficacy and mechanism of action of chitosan nanocapsules for oral peptide delivery. *Pharm Res* 2006;23:549-56.
- Pan Y, Li YJ, Zhao HY, Zheng JM, Xu H, Wei G, *et al.* Bioadhesive polysaccharide in protein delivery system: Chitosan nanoparticles improve the intestinal absorption of insulin *in vivo*. *Int J Pharm* 2002;249:139-47.
- Hasanovic A, Zehl M, Reznicek G, Valenta C. Chitosan-tripolyphosphate nanoparticles as a possible skin drug delivery system for aciclovir with enhanced stability. *J Pharm Pharmacol* 2009;61:1609-16.
- Tan ML, Choong PF, Dass CR. Cancer, chitosan nanoparticles and catalytic nucleic acids. *J Pharm Pharmacol* 2009;61:3-12.
- Chen Y, Zhao YH, Jia XB, Hu M. Intestinal absorption mechanisms of prenylated flavonoids present in the heat-processed *Epimedium koreanum* Nakai (Yin Yanghuo). *Pharm Res* 2008;25:2190-9.
- Tanaka Y, Taki Y, Sakane T, Nadai T, Sezaki H, Yamashita S. Characterization of drug transport through tight-junctional pathway in Caco-2 monolayer: Comparison with isolated rat jejunum and colon. *Pharm Res* 1995;12:523-8.
- Yan HM, Zhang ZH, Jiang YR, Ding DM, Sun E, Jia XB. An attempt to stabilize tanshinone IIA solid dispersion by the use of ternary systems with nano-CaCO₃ and poloxamer 188. *Pharmacogn Mag* 2014;10 Suppl 2:S311-7.
- Turco L, Catone T, Caloni F, Di Consiglio E, Testai E, Stammati A. Caco-2/TC7 cell line characterization for intestinal absorption: How reliable is this *in vitro* model for the prediction of the oral dose fraction absorbed in human? *Toxicol In vitro* 2011;25:13-20.
- Calvo P, Remuñán-López C, Vila-Jato JL, Alonso MJ. Novel hydrophilic chitosan-polyethylene oxide nanoparticles as protein carrier. *J Appl Polym Sci* 1997;63:125-32.
- Jin X, Zhang ZH, Sun E, Tan XB, Zhu FX, Jia XB. A novel drug-phospholipid complex loaded micelle for baohuoside I enhanced oral absorption: *In vivo* and *in vivo* evaluations. *Drug Dev Ind Pharm* 2013;39:1421-30.
- Jin X, Zhang ZH, Sun E, Tan XB, Li SL, Cheng XD, *et al.* Enhanced oral absorption of 20(S)-protopanaxadiol by self-assembled liquid crystalline nanoparticles containing piperine: *In vitro* and *in vivo* studies. *Int J Nanomedicine* 2013;8:641-52.
- Mosmann T. Rapid colorimetric assay for cellular growth and survival: Application to proliferation and cytotoxicity assays. *J Immunol Methods* 1983;65:55-63.
- Chae SY, Jang MK, Nah JW. Influence of molecular weight on oral absorption of water soluble chitosans. *J Control Release* 2005;102:383-94.

22. Jin X, Zhang ZH, Sun E, Qian Q, Tan XB, Jia XB. Preparation of a nanoscale baohuoside l-phospholipid complex and determination of its absorption: *In vivo* and *in vitro* evaluations. *Int J Nanomedicine* 2012;7:4907-16.
23. Jin X. A nanostructured liquid crystalline formulation of 20(S)-protopanaxadiol with improved oral absorption. *Fitoterapia* 2013;84:64-71.
24. Guan M, Zhu QL, Liu Y, Bei YY, Gu ZL, Zhang XN, *et al.* Uptake and transport of a novel anticancer drug-delivery system: Lactosyl-norcantharidin-associated N-trimethyl chitosan nanoparticles across intestinal Caco-2 cell monolayers. *Int J Nanomedicine* 2012;7:1921-30.
25. Dudhani AR, BioKosaraju S.L. Bioadhesive chitosan nanoparticles: Preparation and characterization. *Carbohydr Polym* 2010;81:243-51.
26. Lin YH, Chen CT, Liang HF, Kulkarni AR, Lee PW, Chen CH, *et al.* Novel nanoparticles for oral insulin delivery via the paracellular pathway. *Nano-technology* 2007;18:105102.
27. Kean T, Thanou M. Biodegradation, biodistribution and toxicity of chitosan. *Adv Drug Deliv Rev* 2010;62:3-11.
28. Lian H, Sun J, Yu YP, Liu YH, Cao W, Wang YJ, *et al.* Supramolecular micellar nanoaggregates based on a novel chitosan/vitamin E succinate copolymer for paclitaxel selective delivery. *Int J Nanomedicine* 2011;6:3323-34.
29. Zhou W, Qin KM, Shan JJ, Ju WZ, Liu SJ, Cai BC, *et al.* Improvement of intestinal absorption of forsythoside A in *Weeping forsythia* extract by various absorption enhancers based on tight junctions. *Phytomedicine* 2012;20:47-58.
30. Li YH, Zhang M, Wang JC, Zhang S, Liu JR, Zhang Q. Effects of absorption enhancers on intestinal absorption of lumbrokinase. *Yao Xue Xue Bao* 2006;41:939-44.
31. Wang JJ, Zeng ZW, Xiao RZ, Xie T, Zhou GL, Zhan XR, *et al.* Recent advances of chitosan nanoparticles as drug carriers. *Int J Nanomedicine* 2011;6:765-74.
32. Zhang HL, Zhong XB, Tao Y, Wu SH, Su ZQ. Effects of chitosan and water-soluble chitosan micro- and nanoparticles in obese rats fed a high-fat diet. *Int J Nanomedicine* 2012;7:4069-76.



Ke Liang



Zeng-yong Jia

ABOUT AUTHORS

Ke Liang, is PhD for urology, attending doctor in the First Affiliated Hospital of Soochow University, China. He is interested in oral formulation design and investigations in pharmaceutical field.

Zeng-yong Jia, is an Professor at the Department of Pharmacy, The Suqian First Hospital, China. His research interest is in the area of Nano Pharmaceutics and its evaluation. Additionally, he is also a clinical pharmacist and interested in proper use of clinical medicine.